Effect of Lateral Heat Losses on the Stability of Thermal Displacement Fronts in Porous Media

Previous studies have shown that heat transport by horizontal conduction in thermal displacement processes in porous media has a stabilizing effect on condensation fronts. This paper expands the stability analysis by also including the description of heat transfer lateral heat losses by conjungate (vertical) conduction. A marginal stability condition is derived in terms of a parameter Λ representing the relative magnitude of heat transfer by conjugate conduction. It is shown that lateral heat losses ask a significant stabilizing effect on the front. This effect should be important in thermal oil recovery processes such as steam injection and *in-situ* combustion.

Y. C. YORTSOS

Departments of Chemical and Petroleum Engineering
University of Southern California
Los Angeles, CA 90007

SCOPE

An important class of processes for the recovery of viscous oil from underground oil reservoirs involves the supply of heat either by steam injection or by *in-situ* combustion. The primary objective in such thermal processes is to facillitate recovery by taking advantage of the substantial reduction of oil viscosity obtained at high temperatures. The effectiveness of a thermal recovery project largely depends on two factors: (1) the sustained propagation through the reservoir of high temperature fronts (e.g., steam or combustion fronts) that typically arise in such processes; and (2) the achievement of a high degree of areal coverage (sweep efficiency) by the propagating front. Among other considerations, frontal stability plays a crucial role for the successful implementation of these two conditions.

The stability of moving thermal displacement fronts in porous media was examined by Miller (1975) for the case of adiabatic processes. His results showed that thermal fronts tend to be more stable than isothermal displacement fronts, due to volumetric contraction accompanying phase change and heat transport near the front. Both effects are strongly dependent upon the heat transfer mechanism in the reservoir, and are expected to vary considerably when heat losses to the surroundings are included in the heat transfer model. Lateral heat losses account for a significant portion of the heat injected or generated, and result into front retardation and sharpening of the temperature distribution in the reservoir. In this paper a study is undertaken to investigate the effect to frontal stability caused by heat losses to the surroundings by conjugate (vertical) conduction in a steam injection process. In the analysis we make use of the heat transfer model developed by Yortsos and Gavalas (1979) and the linear stability analysis presented by Miller (1975). The study is restricted to fronts that remain vertical to the reservoir bounding planes, hence the results are expected to be applicable to thin reservoirs.

CONCLUSIONS AND SIGNIFICANCE

Based on a heat transfer model that accounts for convection, conduction, and lateral heat losses to the surrounding formations by conjugate conduction, the stability of moving condensation fronts in steam injection processes is examined. A linear stability analysis predicts that inclusion of lateral heat losses leads to a significant stabilizing effect. The marginal stability condition is expressed in terms of a dimensionless parameter Λ representing the relative magnitude of lateral heat losses. It is shown that the stabilizing contribution increases with a decrease in the steam injection rates (increase in Λ). The analysis indicates that the principal reason for the increase in the frontal stability is the significant reduction in the water velocity accompanying phase change at the front, rather than a purely heat transport effect. The latter asks a stabilizing effect according to the mechanism outlined by Miller (1975). At small values of the length of the perturbation this mechanism is aided by the heat losses. For larger lengths of perturbation, however, conjugate conduction slightly impedes the stabilizing influence asked by heat conduction parallel to the front. The results obtained find application to thermal recovery processes that give rise to traveling condensation fronts (such as steam injection or *in-situ* combustion) in thin reservoirs.

INTRODUCTION

Since the inception of thermal processes for the recovery of heavy oils, the stability of thermal displacement fronts in porous media has been the subject of considerable interest (Baker (1973)). However, only recently a rigorous analysis has been undertaken. Based on a study of the stability of moving surfaces in fluid systems with heat and mass transport (Miller (1973)), Miller (1975) investigated the stability of moving displacement fronts in adiabatic steam injection processes. He proceeded by assuming potential flow in both the steam and the liquid zones adjacent to the moving front, and by neglecting heat losses from the reservoir to the surrounding formations, but otherwise including conductive and convective heat transfer to the liquid zone ahead of the front. Miller's results, which were further extended to in-situ combustion (Armento and Miller (1977)), showed that in addition to the familiar mobility and gravity effects associated with isothermal immiscible displacement (Saffman and Taylor (1958)), steam condensation at the front and

ISSN-0001-1541-82-4500-0480-$2.00.

heat transport in the liquid zone ask significant stabilizing contributions.

An important mode of heat transfer, inherent to any thermal process in an underground oil reservoir, involves heat losses by conjugate conduction to the surrounding the reservoir formations. As pointed out in a previous study (Yortsos and Gavalas (1981)) lateral heat losses cause considerable retardation of front propagation in steam injection processes through an increase of steam condensation, and by sharpening the temperature distribution in the liquid zone. It is anticipated that these effects, particularly heat transport in the liquid zone, would be significant in the stability of the front. An analysis of heat transfer ahead of moving condensation fronts including horizontal convection and conduction, and conjugate (vertical) conduction, was undertaken by Yortsos and Gavalas (1982). Their results are applied in this study in order to assess the contribution of lateral heat losses to the stability of the front.

Throughout the analysis the following assumptions are made: The reservoir is homogeneous and isotropic and is bounded by two parallel planes. The front is assumed to be and to remain vertical to the planes bounding the reservoir, thus the effect of gravity enters insofar as the reservoir is inclined with respect to the horizontal plane (no gravity override of the steam zone is considered). Since this is not generally the case in an arbitrary process, the results to be obtained here are strictly applicable to thin reservoirs, where gravity override is not significant. It is also assumed that heat losses do not affect the flow characteristics, so that we can treat the flow in both the steam and the liquid zones as one-phase, potential flow. Finally, the derivation is presented in dimensionless notation such that a comparison with the results for the case of zero heat losses can follow directly.

MATHEMATICAL FORMULATION

Flat Condensation Front

We consider the stability of a flat condensation front in a rectangular reservoir of thickness h, inclined with respect to the horizontal, and bounded from above and below by impermeable to flow rock strata (Figure 1a). The reservoir is initially at temperature T_i. By virtue of steam injection or some other thermal process, a condensation front of constant temperature T_s develops and propagates along the flow direction at constant velocity v. The reservoir is thereby divided into a region of constant temperature (steam zone) and a zone of varying temperature (liquid zone). At any stage during the process, steam flows in the steam zone at constant velocity u_s, and condenses at the steam front to water. The latter flows through the moving front and inside the liquid zone at constant velocity u_w. Side by side with the fluid flow in the liquid zone, heat flows by horizontal conduction and convection in the reservoir and by vertical conduction to the surroundings (lateral heat losses).

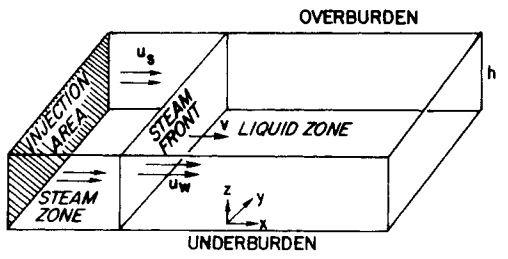

a. Before Perturbation

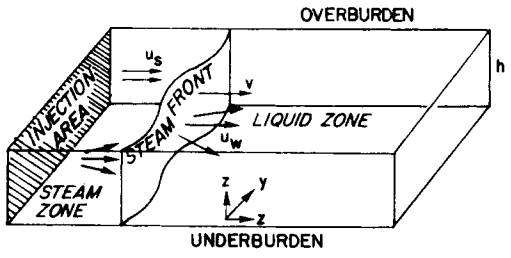

b. After Perturbation

Figure 1. Reservoir description.

Heat Transfer in the Liquid Zone. Assuming uniform properties, the temperature distribution in the hot liquid zone is described by the integrodifferential equation (Yortsos and Gavalas, 1982)

$$M\frac{\partial T}{\partial t}+u_w\rho_w C_{pw}\frac{\partial T}{\partial x}=k_{hR}\frac{\partial^2 T}{\partial x^2}-\frac{2k_{hf}}{h\sqrt{\pi\alpha_f}}\int_0^t\frac{\partial T}{\partial\tau}\frac{d\tau}{\sqrt{t-\tau}} \quad (1)$$

Equation 1 allows for horizontal convection and conduction, and lateral heat losses by conjugate conduction (last term on the RHS). In terms of the dimensionless variables (denoted by subscript D)

$$T_D=\frac{T-T_i}{T_s-T_i},\quad x_D=\left(\frac{k_{hR}\Delta T}{\rho_s L_v u_s}\right)^{-1}x,\quad t_D=\left(\frac{k_{hR}\Delta TM}{u_s^2\rho_s L_v\rho_w C_{pw}}\right)^{-1}t \quad (2)$$

Equation 1 becomes

$$\frac{\partial T_D}{\partial t_D}+\frac{u_{wD}}{m}\frac{\delta T_D}{\delta x_D}=\frac{1}{\gamma \mathrm{St}}\frac{\partial^2 T_D}{\partial x_D^2}-\frac{\sqrt{\Lambda}}{\sqrt{\pi}}\int_0^{t_D}\frac{\partial T_D}{\partial\tau_D}\frac{d\tau_D}{\sqrt{t_D-\tau_D}} \quad (3)$$

In the above, M is the volumetric heat capacity of the liquid zone, L_v the latent heat of condensation, ΔT the difference between injected and initial temperature, γ the ratio of water to steam densities, St the Stefan number $\mathrm{St}=(C_{pw}\Delta T)/L_v$, and m the ratio of the volumetric heat capacities $m=M/(\rho_w C_{pw})$. The dimensionless parameter Λ expresses the relative magnitude of the rate of heat transfer by vertical conduction to the rate of heat transfer by horizontal convection

$$\Lambda=\frac{4k_{hf}^2 k_{hR}\Delta T}{h^2 M\alpha_f\rho_s L_v\rho_w C_{pw}u_s^2} \quad (4)$$

In case of negligible heat losses ($k_{hf}=0$), $\Lambda=0$ (Miller, 1975). At steady-state, in the moving coordinates t_D, $\xi_D=x_D-v_D t_D$, Eq. 3 becomes (Yortsos and Gavalas, 1982)

$$\left(\frac{u_{wD}}{m}-v_D\right)\frac{\partial T_D}{\partial\xi_D}=\frac{1}{\gamma \mathrm{St}}\frac{\partial^2 T_D}{\partial\xi_D^2}+\frac{\sqrt{\Lambda}\sqrt{v_D}}{\sqrt{\pi}}\int_0^{\infty}\frac{\partial T_D(\sigma+\xi_D)}{\partial\sigma}\frac{d\sigma}{\sqrt{\sigma}} \quad (5)$$

At steady-state, the temperature distribution in the liquid zone follows as a solution of Eq. 5 along with boundary conditions

$$T_D=1;\quad \xi_D=0 \quad (5a)$$

$$T_D=0;\quad \xi_D\to\infty \quad (5b)$$

One obtains

$$T_D=\exp[-z_1\xi_D] \quad (6)$$

where z_1 satisfies the albegraic equation

$$z_1\left(\frac{z_1}{\gamma \mathrm{St}}+\frac{u_{wD}}{m}-v_D\right)^2=\Lambda v_D \quad (7)$$

The parameter z_1 represents a dimensionless temperature gradient at the condensation front and, for fixed injection and reservoir conditions, can be determined in terms of u_{wD}, v_D. The latter are obtained from mass and heat balances at the front.

TABLE 1. TYPICAL VALUES OF RESERVOIR PARAMETERS FOR STEAM INJECTION

Parameter	Unit	Values
C_{pw}, specific heat	kJ/kg · K	4.186
ϵ, porosity	—	0.345
h, thickness	m	25.4
k_h, thermal conductivity	W/m · K	2.768
L_v, latent heat	MJ/kg	1.79
M, volumetric heat capacity	MJ/m^3 · K	2.722
ρ_w, density	kg/m^3	823.31
ρ_s, density	kg/m^3	14.77
$\rho_f C_{pf}$, volumetric heat capacity	MJ/m^3 · K	2.345
T_i, temperature	°C	30
T_s, temperature	°C	236
u_s, steam flow rate	m/s	0.000056

Conditions at the Front. From the water mass balance across the front

$$\rho_s u_s - \rho_w u_w = \epsilon v(\rho_s - \rho_w) \tag{8}$$

we obtain in dimensionless notation

$$u_{wD} - \epsilon\left(1 - \frac{1}{\gamma}\right) v_D = \frac{m}{\gamma}, \tag{8a}$$

where ϵ is the porosity of the reservoir. Similarly from the heat balance across the front

$$k_{hR}\left(-\frac{\partial T}{\partial x}\right) = \rho_s L_v(u_s - \epsilon v) \tag{9}$$

we have

$$\frac{\epsilon}{m} v_D + z_1 = 1. \tag{9a}$$

Expressions 7, 8a, 9a define z_1, u_{wD}, v_D uniquely in terms of the parameters Λ, St.

For later convenience, it is useful to denote the ratio of the temperature gradient z_1 to the corresponding value for the case of zero heat losses z_1° by

$$w = \frac{z_1}{z_1^\circ} \tag{10}$$

Here z_1° is determined from Eqs. 7, 8a, 9a by setting $\Lambda = 0$. Then,

$$z_1^\circ = \left(\frac{m}{\epsilon} - 1\right) \Big/ \left[\frac{m}{\epsilon} - 1 + \frac{1}{\gamma}\left(\frac{1}{\mathrm{St}} + 1\right)\right] \tag{10a}$$

and w is the solution of the equation

$$w(w-1)^2\left(\frac{m}{\epsilon} - 1\right)^2 = \left(\frac{1}{z_1^\circ} - w\right)\frac{m}{\epsilon}\Lambda. \tag{10b}$$

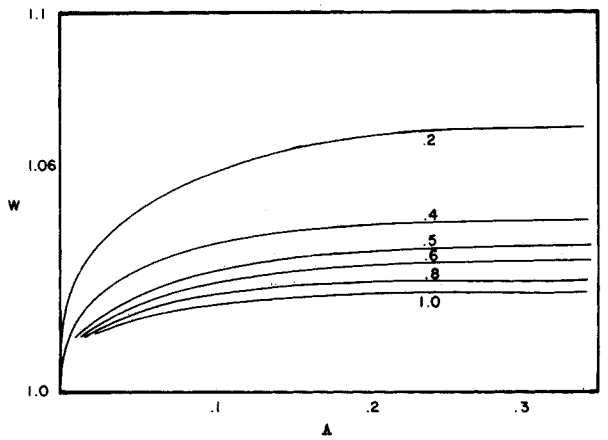

Figure 2. Ratio of temperature gradients w vs. Λ for various values of St.

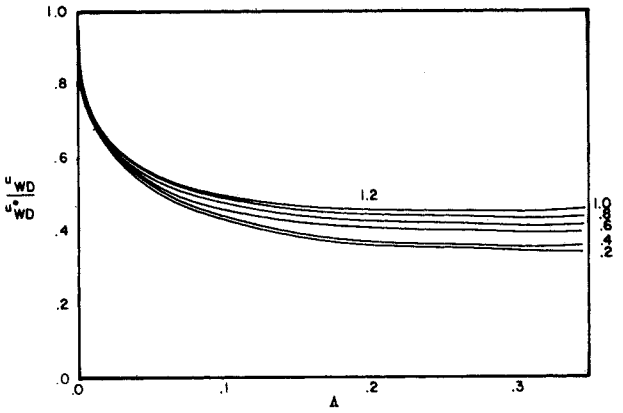

Figure 3. Ratio of water flow rates vs. Λ for various values of St.

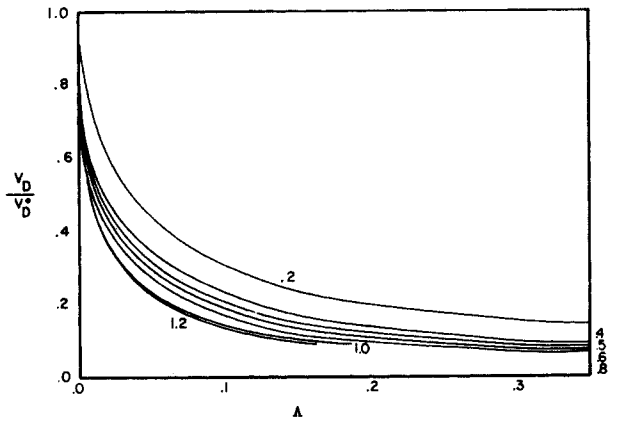

Figure 4. Ratio of front velocities vs. Λ for various values of St.

The ratios z_1/z_1°, u_{wD}/u_{wD}°, v_D/v_D° are plotted vs. Λ for typical values of the reservoir parameters (Table 1) on Figures 2, 3, 4 respectively. As shown in Figure 2 the gradient at the front although increasing with Λ does not vary considerably. At large values of Λ it approaches $1 + [(1/\mathrm{St}) + 1]/\gamma[(m/\epsilon) - 1]$ which for typical values of the reservoir parameters is equal to 1.069. By contrast, the water flow rate and the front velocity are drastically decreased by an increase in Λ (Figures 3 and 4). As Λ increases, the water flow rate quickly approaches the asymptotic value $[m/\epsilon - 1 + 1/\gamma(1/\mathrm{St} + 1)]/(m/\epsilon + 1/\mathrm{St})$, which for typical values of the reservoir parameters is equal to 0.313. Similarly, the front velocity is a decreasing function of Λ and asymptotically reduces to zero at large Λ.

Stability Analysis

We proceed with a linear stability analysis following the approach outlined by Miller (1975). The condensation front, initially the plane $\xi_D = 0$, is presumed to undergo a small perturbation to the position $\xi_D = \delta(t)f(y_D)$, (Figure 1b), where the dimensionless wave form function satisfies the equation

$$\frac{\partial^2 f}{\partial y_D^2} = -\alpha_D^2 f, \tag{11}$$

and the dimensionless wave number α_D is related to a mean wavelength of perturbation Λ through $\alpha_D = 2\pi/\lambda_D$. Note that the front remains uniformly vertical to the bounding planes after the onset of the perturbation. We further assume that the forms of the perturbations θ_D in temperature and Φ_D in the velocity potential are taken as products of $f(y_D)$ and appropriate functions θ_D and ϕ_D of the distance from the front. Invoking continuity and postulating potential flow in both the steam and the hot liquid zone we obtain

$$\phi_{sD} = a_s f e^{\alpha_D \xi_D}, \tag{12a}$$

$$\phi_{wD} = a_w f e^{-\alpha_D \xi_D}, \tag{12b}$$

for steam and water respectively. The velocity perturbations, denoted by superscript $\sim$, can be obtained from Eq. 12 and use of Darcy's law (Bear (1972))

$$\underline{v}_{iD} = \nabla \phi_{iD}, \quad (i = s,w). \tag{13}$$

The temperature perturbation in the liquid zone is obtained from the heat transfer Eq. 3. After the onset of perturbation the temperature has the form

$$\tilde{T}_D(t_D,\xi_D,y_D) = T_D(\xi_D) + \theta_D(t_D,\xi_D) f(y_D) \tag{14}$$

At marginal stability in moving coordinates Eq. 3 becomes

$$\left(\frac{1}{m}(u_{wD} + \underline{v}_{wD}) - v_D \underline{i}\right) \nabla \tilde{T}_D = \frac{1}{\gamma \mathrm{St}} \nabla^2 \tilde{T}_D + \frac{\sqrt{\Lambda}}{\sqrt{\pi}} \sqrt{v_D} \int_0^\infty \frac{\partial \tilde{T}_D}{\partial \sigma}(\sigma + \xi_D, y_D) \frac{d\sigma}{\sqrt{\sigma}} \tag{15}$$

Expanding to first order in perturbation we further obtain

$$\left(\frac{u_{wD}}{m} - v_D\right) f \frac{\partial \theta_D}{\partial \xi_D} + \frac{v_{wD\xi}}{m} \frac{\partial T_D}{\partial \xi_D} = \frac{f}{\gamma \mathrm{St}} \left[\frac{\partial^2 \theta_D}{\partial \xi_D^2} - \alpha_D^2 \theta_D\right] + \frac{\sqrt{\Lambda}}{\sqrt{\pi}} \sqrt{v_D} f \int_0^\infty \frac{\partial \theta_D(\sigma + \xi_D)}{\partial \sigma} \frac{d\sigma}{\sqrt{\sigma}} \tag{16}$$

Substituting in Eq. 16 the expressions for the original temperature distribution T_D (Eq. 6), and the velocity perturbation $v_{wD\xi}$ from Eqs. 12 and 13, we further obtain

$$\left(\frac{u_{wD}}{m} - v_D\right) \frac{\partial \theta_D}{\partial \xi_D} + \frac{\alpha_D a_w z_1}{m} \exp\{-(\alpha_D + z_1)\xi_D\} = \frac{1}{\gamma \mathrm{St}} \left[\frac{\partial^2 \theta_D}{\partial \xi_D^2} - \alpha_D^2 \theta_D\right] + \frac{\sqrt{\Lambda}}{\sqrt{\pi}} \sqrt{v_D} \int_0^\infty \frac{\partial \theta_D(\sigma + \xi_D)}{\partial \sigma} \frac{d\sigma}{\sqrt{\sigma}} \tag{17}$$

The solution of Eq. 17 which vanishes far from the front is given within the arbitrary constants a,a_w by

$$\theta_D = a \exp\{-r\xi_D\} + \frac{ba_w}{m} \exp\{-(\alpha_D + z_1)\xi_D\}. \tag{18}$$

Here r satisfies the algebraic equation

$$\frac{r^2}{\gamma \mathrm{St}} + r\left(\frac{u_{wD}}{m} - v_D\right) - \sqrt{\Lambda}\sqrt{v_D}\sqrt{r} - \frac{\alpha_D^2}{\gamma \mathrm{St}} = 0, \tag{19}$$

and b is fixed by the expression

$$b = \frac{\alpha_D z_1}{\left[\frac{(\alpha_D + z_1)^2}{\gamma \mathrm{St}} + \left(\frac{u_{wD}}{m} - v_D\right)(\alpha_D + z_1) - \sqrt{\Lambda}\sqrt{v_D}\sqrt{\alpha_D + z_1} - \frac{\alpha_D^2}{\gamma \mathrm{St}}\right]} \tag{20}$$

The marginal stability conditions follows by application of continuity and conservation relations at the front (Miller, 1975). We obtain the following conditions:

(i) Continuity of temperature

$$-\delta z_1 + a + \frac{ba_w}{m} = 0 \tag{21a}$$

(ii) Continuity of pressure

$$\delta\left(1 - \frac{\mu_w k_s}{\mu_s k_w} \frac{u_{wD}}{m} + (\rho_w - \rho_s) g \xi \frac{k_s}{\mu_s u_s}\right) = -\frac{a_s}{m} + \frac{\mu_w k_s}{\mu_s k_w} \frac{a_w}{m} \tag{21b}$$

(iii) Conservation of mass

$$a_w + \frac{1}{\gamma} a_s = 0 \tag{21c}$$

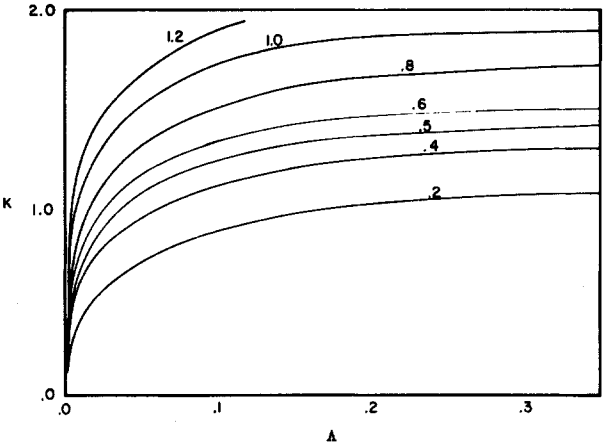

Figure 5. Parameter K vs. Λ for various values of St.

(iv) Conservation of energy

$$-\delta z_1^2 + ra + \frac{ba_w}{m}(\alpha_D + z_1) = \alpha_D \frac{a_s}{m} \tag{21d}$$

Equations 21 form a linear, homogeneous system in the four unknowns a,a_s,a_w,δ. A nontrivial solution exists provided that its determinant is zero. We obtain

$$\left[1 - \frac{\mu_w k_s}{\mu_s k_w} \frac{u_{wD}}{m}\right] + \frac{(\rho_w - \rho_s) g_\xi k_s}{\mu_s u_s} + \left[1 + \frac{\mu_w k_s \rho_s}{\mu_s k_w \rho_w}\right] \times \frac{z_1(r - z_1)/\alpha_D}{\left[1 + \frac{b}{\gamma}\left(1 + \frac{z_1}{\alpha_D} - \frac{r}{\alpha_D}\right)\right]} = 0 \tag{22}$$

Expression 22 constitutes the final form of the marginal stability condition. The first two terms in Eq. 22 represent mobility and gravity effects on the stability of the front, while the third term accounts for heat transport to the liquid zone and heat losses by conjugate conduction to the surroundings.

To simplify Eq. 22 we introduce a normalized length of perturbation $\sigma = z_1^2/\alpha_D$ and a normalized perturbation temperature gradient $\zeta = r/\alpha_D w$. By direct substitution in Eq. 19 it follows that ζ satifies the algebraic equation

$$\zeta^2 - \zeta\sigma + K(\zeta\sigma - \zeta^{1/2}\sigma^{3/2}) - \frac{1}{w^2} = 0, \tag{23}$$

where the dimensions parameter K is defined by

$$K = \frac{\sqrt{v_D}\sqrt{\Lambda}\,\gamma \mathrm{St}}{z_1^{3/2}} \tag{24}$$

Figure 5 shows K plotted vs. Λ for various of St and typical reservoir conditions. At larger values of Λ the parameter K approaches the asymptotic value 1 + St. Notice that in the case of zero heat losses ($\Lambda = 0$, $w = 1$, $K = 0$), Eq. 23 reduces to the dimensionless quadratic

$$\zeta^2 - \zeta\sigma - 1 = 0 \tag{25}$$

use of which was previously made by Miller (1975).

In terms of the normalized variables σ,ζ the marginal stability condition 22 takes the final form

$$-\left[1-\frac{\mu_w k_s}{\mu_s k_w}\frac{u_{wD}}{m}\right]-\frac{(\rho_w-\rho_s)g_\xi k_s}{\mu_s u_s}-\left[1+\frac{\mu_w k_s \rho_s}{\mu_s k_w \rho_w}\right]$$

$$\times\left\{\frac{z_1^{\circ} w^2(\zeta-\sigma)}{\left[1+\dfrac{\mathrm{St}[\sigma-\zeta+1/w]}{1/w+K[\sigma+1/w-\sigma^{1/2}\sqrt{\sigma+1/w}]}\right]}\right\}=0 \quad (26)$$

For simplicity of discussion we denote the quantity in brackets by

$$I=\frac{z_1^{\circ} w^2(\zeta-\sigma)}{\left\{1+\dfrac{\mathrm{St}[\sigma-\zeta+1/w]}{1/w+K[\sigma+1/w-\sigma^{1/2}\sqrt{\sigma+1/w}]}\right\}} \quad (27)$$

The dependence of Eq. 26 on Λ which is the primary quantity of interest here, enters through the expressions for u_{wD}, w, ζ and K. For the case of zero heat losses ($\Lambda = 0$), expression 26 reduces to the normalized form

$$-\left[1-\frac{\mu_w k_s}{\mu_s k_w}\frac{u_{wD}^{\circ}}{m}\right]-\frac{(\rho_w-\rho_s)g_\xi k_s}{\rho_s u_s}$$

$$-\left[1+\frac{\mu_w k_s \rho_s}{\mu_s k_w \rho_w}\right]\frac{z_1^{\circ}(\zeta-\sigma)}{\{1+\mathrm{St}(\sigma-\zeta+1)\}}=0 \quad (28)$$

previously derived by Miller (1975).

RESULTS AND DISCUSSION

The contribution to the frontal stability of each of the three terms in Eq. 26 has been outlined by Miller (1975). For given injection and reservoir conditions, a term asks a stabilizing effect if its value is negative, and a destabilizing effect if its value is positive.

Due to the negative difference in density between injected and displaced fluids, the second term representing gravity effects has a stabilizing contribution to the front, equal in magnitude to the contribution in the case of zero heat losses. (Compare Eq. 26 to 28.) Similarly, due to contraction in volume accompanying the phase change at the front, fluid mechanical effects (first term in Eq. 26) exert a more stabilizing influence on the front than in the case of isothermal, immiscible displacement. Owing to conjugate conduction, however, the water velocity u_{wD} is considerably smaller, for typical values of Λ, than its value u_{wD}° in the case of zero heat losses (Figure 3). (It should be noted that the dimensionless quantity u_{wD}/m in Eqs. 26 and 28 is equal to u_w/u_s.) This reduction in the water flow rate, which may reach a value as low as 0.31 of u_{wD}°, adds favorably to the stability of the front. In fact, as discussed below, it represents the main effect heat losses have on frontal stability.

The third term in Eq. 26 accounts for heat transport ahead of the front by horizontal conduction and convection and in a direction normal to the reservoir by conjugate conduction. Figure 6 shows the heat transport term I plotted vs. σ for various values of Λ. As shown in Figure 6 this term asks a stabilizing effect for any value of the perturbation length. The contribution is greater at small values of σ and becomes smaller as σ increases. Contrary to what one might expect, however, this contribution is smaller than in the case of zero heat losses and it is decreasing with an increase in Λ to an asymptotic positive limit at large Λ, for all σ outside a narrow region near the origin. This region (not shown in Figure 6) covers the span $0 < \sigma < 0.13$ for typical values of the reservoir parameters. For values of σ within the narrow region, corresponding to values of the perturbation length that do not exceed a small fraction of the characteristic distance within which the temperature of the liquid zone drops to its initial value, enhancement of stability due to heat transport is higher as Λ increases, although it does not exceed a maximum of approximately 1.069 of its value when $\Lambda = 0$. (Compare with Eq. 10.)

Thus, heat transport adds favorably to frontal stability although by a lesser degree than in the case $\Lambda = 0$, except for a narrow region corresponding to small values of the perturbation length. It should

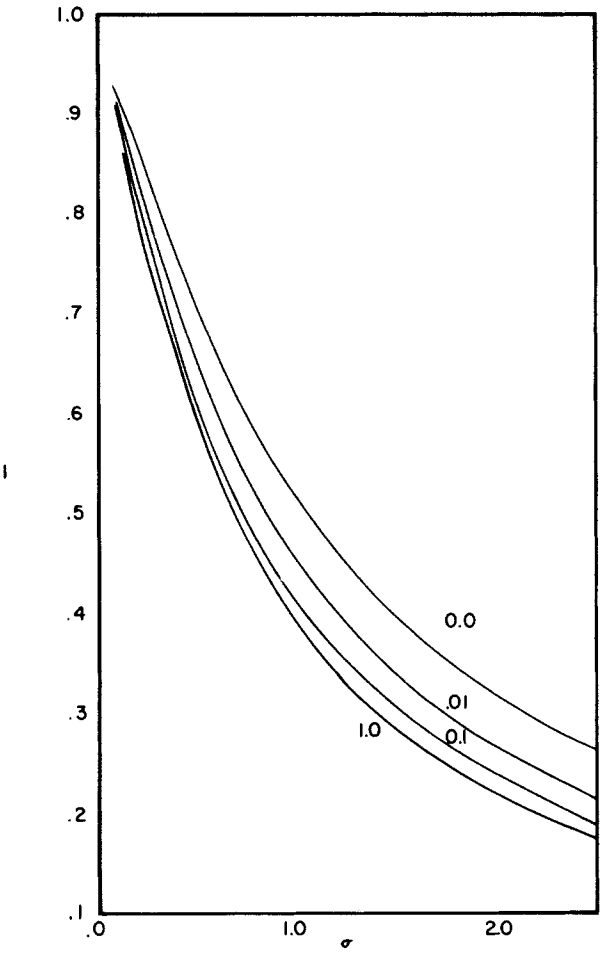

Figure 6. Heat transport term I vs. σ for various values of Λ.

be remarked that similar results are also obtained when the heat losses are modeled by the conventional but less realistic mode of convective cooling, i.e., (rate of heat losses) $\propto (T - T_i)$. A simple explanation of this behavior can be furnished by the following argument. As Λ increases, the temperature gradient in a direction normal to the front increases. Thus, the heat penetration depth decreases. Similarly, at sufficiently large lengths of perturbation (sufficiently small front curvature), the temperature gradient in a direction parallel to the front decreases. Therefore, the stabilizing mechanism due to heat transport parallel to the front (Miller, 1975), although still in effect, is hampered as Λ increases resulting into a smaller stabilizing effect. It should be added that since we did not consider in the heat transfer model heat conduction in the surroundings in a direction parallel to the reservoir bounding plane, the actual effect of lateral heat losses should be slightly more stabilizing.

The combined effect of the first and third terms on the marginal stability is shown in Figure 7 for various values of Λ and for two different values of the mobility ratio. The marginal stability curves divide the space into two regions, a stability region to the right side of each curve and an instability region to the left. It is shown that the overall effect of heat losses is to enhance considerably the stability of the front, even for relatively low values of Λ. This effect is more pronounced at higher values of the mobility ratio. Similar conclusions can be drawn from Figure 8 where the dimensionless wave number is plotted vs. St for various values of Λ, under typical reservoir conditions. The critical wave number α_{crit} below which instability sets off can be directly evaluated under typical conditions: For St = 0.5, mobility ratio equal to 20, and $\Lambda = 0$, $\alpha_{crit} = 6.75 \times 10^{-2}(\mathrm{m}^{-1})$ while $\alpha_{crit} = 4.96 \times 10^{-2}(\mathrm{m}^{-1})$ for $\Lambda = 0.001$. Similarly, for mobility ratio equal to 40, the corresponding values are $1.12(\mathrm{m}^{-1})$ and $6.70 \times 10^{-1}(\mathrm{m}^{-1})$, respectively. For completeness, the effect of the injection rate on the marginal stability was

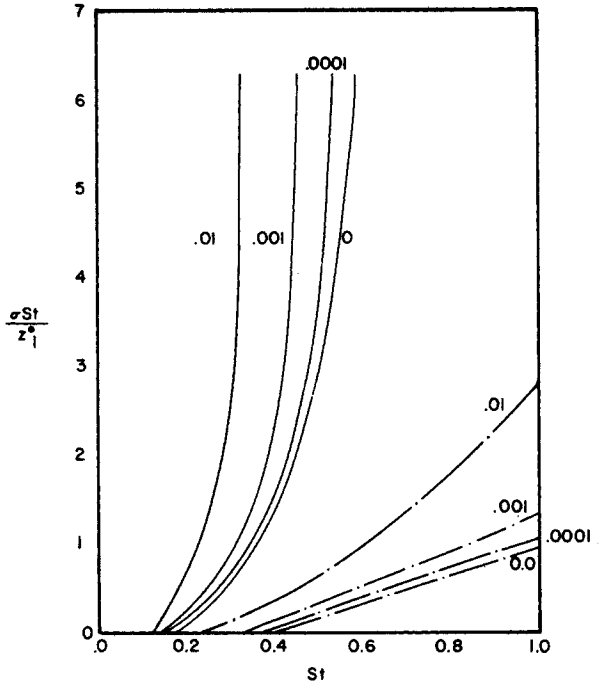

Figure 7. Marginal stability curve for various values of Λ and mobility ratio equal to 20 (solid lines) and 40 (dashed lines).

also investigated (Figure 9). Using typical values (Table 1) and for two different values of the mobility ratio, the stability curve is plotted in a $1/\alpha$ vs. St diagram for different steam flow rates. It is observed that high flow rates tend to destabilize the front, in accordance with the above and the fact that higher steam velocities result into smaller values of Λ.

The foregoing discussion confirms the intuitive hypothesis that heat losses have an overall positive contribution to frontal stability.

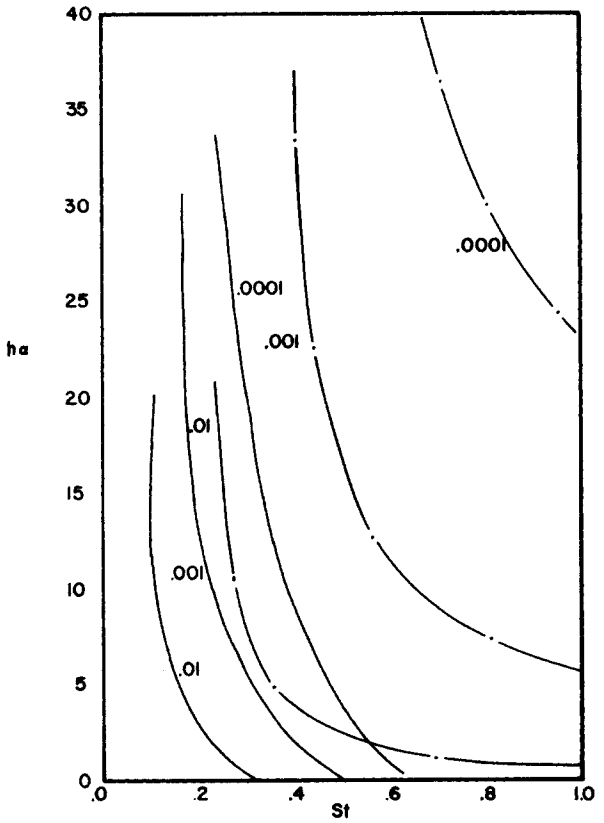

Figure 8. Marginal stability curve for various values of Λ and mobility ratio equal to 20 (solid lines) and 40 (dashed lines).

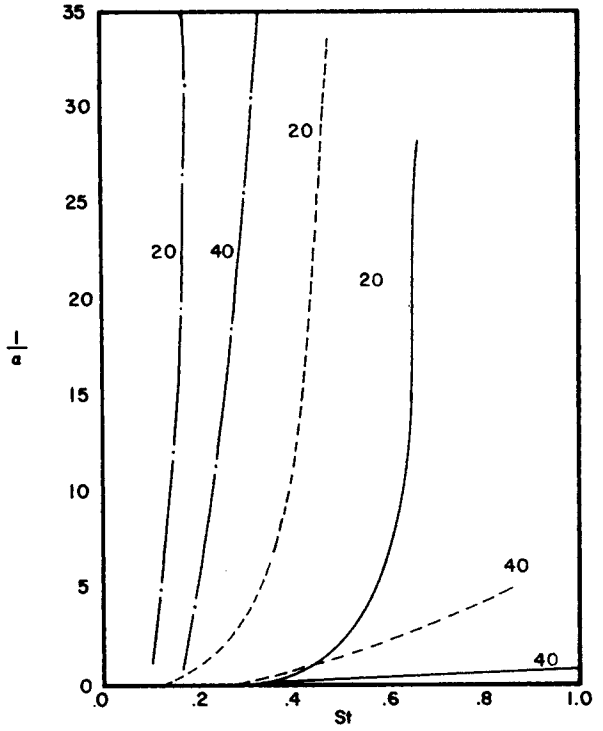

Figure 9. Marginal stability curve: $1/\alpha(m)$ vs. St, for mobility ratio values 20, 40 and $u_s = 1.477 \times 10^{-5}$ kg/m² · s (dotted lines). $u_s = 1.477 \times 10^{-4}$ kg/m² · s (dashed lines), $u_s = 1.477 \times 10^{-3}$ kg/m² · s (solid lines)

This contribution can be quite significant under typical values of the injection parameters ($\Lambda = 10^{-3}$ to 10^{-2}). Even more stable fronts are to be expected for lower values of the steam injection rates. As indicated, the main cause for the increased stability should be attributed to the significant reduction in the water velocity experienced by volumetric contraction at the front, which counterbalances the slight decrease associated with the heat transport team. The conclusions reached here are strictly applicable to processes involving vertical fronts and perturbation such that the fronts remain uniformly vertical to the bounding planes (as is the case in thin reservoirs). Therefore, they cannot be directly applicable to processes exhibiting significant gravity override by the steam zone. For the latter case, a more extensive analysis is requried.

ACKNOWLEDGMENT

The author wishes to thank Andrew Bin Huang for providing considerable help in the numerical calculations and participating in helpful discussions.

NOTATION

b = parameter defined by Eq. 20, dimensionless
C_p = specific heat, $[L^2t^{-2}T^{-1}]$
f = perturbation function, dimensionless
h = reservoir thickness, $[L]$
k = permeability, $[L^2]$
k_h = thermal conductivity, $[MLt^{-3}T^{-1}]$
K = parameter defined by Eq. 24, dimensionless
L_v = latent heat of vaporization, $[L^2t^{-2}]$
m = ratio of volumetric heat capacities, dimensionless
M = volumetric heat capacity, $[ML^{-1}t^{-2}]$
r = parameter defined by Eq. 19, dimensionless
St = Stefan number, dimensionless
t = time, $[t]$
T = temperature, $[T]$

u = flow rate per unit area, $[Lt^{-1}]$
v = front velocity, $[Lt^{-1}]$
w = parameter defined by Eq. 10b, dimensionless
x = space coordinate, $[L]$
y = space coordinate, $[L]$
z = space coordinate, $[L]$
z_1 = parameter defined by Eq. 7, dimensionless

Greek Letters

α = wave number, $[L^{-1}]$
γ = density ratio, dimensionless
δ = amplitude of front displacement, dimensionless
ϵ = porosity, dimensionless
ζ = normalized temperature gradient, dimensionless
θ = perturbation in temperature, dimensionless
Λ = heat transfer parameter, dimensionless
μ = viscosity, $[ML^{-1}t^{-1}]$
ξ = space coordinate, $[L]$
ρ = density, $[ML^{-3}]$
σ = normalized perturbation length, dimensionless
ν = perturbation in velocity, dimensionless
ϕ = perturbation in velocity potential, dimensionless

Subscripts

D = dimensionless
f = surrounding formations
i = initial
R = reservoir
s = steam
w = water

Superscripts

o = referring to zero heat losses
$\sim$ = referring to perturbed quantities

LITERATURE CITED

Armento, M. E., and L. A. Miller, "Stability of Moving Combustion Fronts in Porous Media," *Soc. Pet. Eng. J.*, **17**, 423 (1977).

Baker, P. E., "Effect of Pressure and Rate on Steam Zone Development in Steamflooding," *Soc. Pet. Eng. J.*, **13**, 274 (1973).

Bear, J., *Dynamics of Fluids in Porous Media*, Elsevier, New York (1972).

Miller, C. A., "Stability of Moving Surfaces in Fluid Systems with Heat and Mass Transport. II: Combined Effects of Transport and Density Difference Between Phases," *AIChE J.*, **19**, 909 (1973).

———, "Stability of Moving Surfaces in Fluid Systems with Heat and Mass Transport. III: Stability of Displacement Fronts in Porous Media," *AIChE J.*, **21**, 474 (1975).

Saffman, P. G., and G. I. Taylor, "The Penetration of a Fluid into a Porous Medium or Hele-Shaw Cell Containing a More Viscous Liquid," Proc. Roy. Soc. (London), **A245**, 312 (1958).

Yortsos, Y. C., and G. R. Gavalas, "Heat Transfer Ahead of Moving Condensation Fronts in Thermal Oil Recovery Processes" *Int. J. Heat Mass Transfer*, **25** 3, 305 (1982).

———, "Analytical Modeling of Oil Recovery by Steam Injection. Part 2: Asymptotic and Approximate Solutions," *Soc. Pet. Eng. J.*, **21**, 179 (1981).

Manuscript received December 8, 1980; revision received June 23, and accepted July 14, 1981.

Finite Difference Calculation of Current Distributions at Polarized Electrodes

The changing geometry of electrodes undergoing electrodeposition or dissolution can be simulated by successive solutions of Laplace's equation with nonlinear boundary conditions. To overcome the instability in the finite-difference calculation caused by nonlinear boundary conditions, a weighting algorithm to compute the new surface potential on successive iterations has been developed.

G. A. PRENTICE
and
C. W. TOBIAS

Lawrence Berkeley Laboratory and Department of Chemical Engineering, University of California, Berkeley, CA 94720

SCOPE

In electrochemical reactors distribution of reaction rates on the electrode surfaces depends on cell geometry, electrolyte conductivity, charge transfer reaction kinetics, and on the rates of transport of reactants and products to and from reaction sites. The local reaction rate is proportional to the normal flux (current density) at that point. Determination of the potential field in the cell yields the distribution of the electric flux, and hence the distribution of reaction rates.

Except for the simplest of geometries and of kinetic, and mass-transfer conditions, problems of current distribution may be solved only through numerical techniques. This is particularly evident if one considers systems in which the electrode geometry changes as a result of the progress of the surface reaction.

The calculation of local reaction rates at electrode surfaces is generally the crucial step in modeling electrochemical systems. This implies that one must first compute potential and concentration distributions from which the local current densities can be obtained. In general, this problem requires the solution of multi-dimensional partial differential equations with nonlinear boundary conditions, which cannot be solved by elementary analytical techniques, unless simplifying assumptions are invoked. For example, if the electrodes are assumed to be at fixed potentials, and the cell is of a standard symmetric design, the current distribution can be obtained directly from a solution of the classical Dirichlet problem.

The first systematic study of current distribution problems

G. A. Prentice is presently at the Department of Chemical Engineering, The Johns Hopkins University, Baltimore, MD 21218.

ISSN-0001-1541-82-4282-0486-$2.00.